

AC/DC Power Flow modelled with the Flexible General Branch Model and solved with the Holomorphic Embedding Method

Josep Fanals Batllori
u1946589@campus.udg.edu

Abstract—This paper covers the fundamental formulation regarding the combination of a Flexible General Branch Model (FGBM) with the holomorphic embedding method. The FGBM defines the links between buses with a common and complete model which not only works for AC networks but is also useful for DC grids and the conversion types of currents. It has proven to be a successful choice along with the Newton-Raphson method.

The holomorphic embedding method is a non-iterative totally reliable algorithm with a potential edge in comparison to the traditional iterative algorithms. Up to this point in time, it has been used for AC grids and DC components, but no work in the literature covers the AC/DC power flow. This paper establishes the bases for exactly that and shows its applicability in a simple two-bus system.

Index Terms—power flow, holomorphic embedding, AC/DC, convergence, rectifier, inverter

I. INTRODUCTION

The current European power systems are about to undertake massive changes due to EU's policies, which are concerned with the security of energy supply, the competitiveness of electricity markets and the sustainability aspect. Supergrids are being created in order to accommodate this incoming evolution. They use Voltage Source Converters (VSC) and HVDC grids, apart from the current AC system. HVDC offers great flexibility of operation as well as the possibility of multiterminal configurations [1].

Due to that, the modern supergrid will include a considerable percentage of renewable energy sources, like solar power and wind power choices. Specially in Europe, the concept of offshore wind power has been studied in depth [2].

Therefore, it is critical to work with a flexible model of the grid while solving the power flow with reliable tools. The FGBM is detailed in [3]. The authors depict the proposed model and employ it to solve successfully a multiterminal DC grid that connects with AC systems. However, the usage of the NR method could yield infeasible results. On the other hand, the holomorphic embedding method obtains the feasible solution when it exists. It also grants extra information with tools like Sigma and Thévenin approximants.

The holomorphic embedding method is a novel technique that first appeared in [4] as a revolutionary algorithm based on complex analysis, algebraic curves and approximation theory. It has been used for AC power flow analysis as well as for DC components such as diodes or solar panels. Despite that, the state of art does not cover the conversion between AC/DC

grids. It is possible that the tools in which the holomorphic embedding method is based could be extended to the supergrid of the future accompanied by VSC, HVDC, FACTS and overall an increasing number of power electronics elements.

This paper is structured as follows: Section II presents the equations involved in a simple two-bus system; Section III embeds these equations and presents the algorithm that has to be followed; Section IV shows the results obtained and discusses them; finally, Section V concludes the paper.

II. FORMULATION

A simple system such as the one in Figure 1 is selected in order to introduce the adaptation of the holomorphic embedding method to solve the AC/DC power flow.

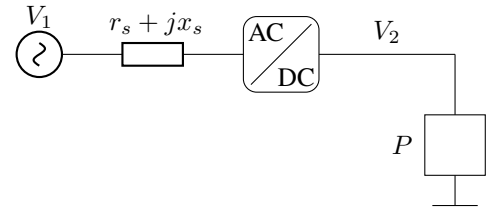


Fig. 1. Simplified system with the AC/DC converter

The slack bus is represented by V_1 , which is known. The reference is established in this exact same bus. The FGBM allows the reference to only be set in a single bus and not having to decouple between AC and DC systems. The most complete FGBM model is employed for the VSC, which links an AC bus with a DC bus, or rather, a DC bus with an AC bus, since the DC bus is indexed by f (from) and the AC one with t (to).

Once the converter is surpassed, the connections between DC buses would obey the traditional model that integrates a single resistance, i.e. $x_s = 0$ and $b_c = 0$. There is no further complication on this side of the system. In this case, only a constant power load has been placed. The hardest part to model is found in the conversion from AC to DC. According to [3], in each DC network there has to be a single type II converter (it could also be a type III). The remaining converters follow the type I constraints. Due to that, in this example the only converter will be type II, and more in depth, the control mode number 5 is applied.

Therefore, the DC voltage will be known (not its phase, only its absolute value) and also the AC bus. Indeed, the slack bus is not treated as an unknown. Usually, three variables emerge from every converter: θ_{sh} , m_a and B_{eq} . Fortunately, $\theta_{sh} = 0$ and $m_a = 1$ due to the fact that the only controlled variable is V_2 , or rather, v_{dc} .

Quite straightforwardly, the first equation to derive connects the current I_f (the one leaving the DC bus in direction to the slack bus) with the whole system:

$$I_f = y_s(V_2 - V_1) + j\frac{b_c}{2}V_2 + jB_{eq}V_2 + G|I_f|^2V_2, \quad (1)$$

where several changes of variables were introduced. $G = \frac{G_0}{I_{f,nom}^2}$ and $y_s = \frac{1}{r_s + jx_s}$. The equation results from the admittance matrix taking into account the aforementioned values of the converter.

The next equation to take into account has to do with the constant complex power load located in the DC side of the system. The beauty of this methodology is found in that all voltages and currents are complex variables, yet reactive power disappears because the DC phases match (or are rotated π radians). Thus

$$P + 0j = V_2 I_f^*. \quad (2)$$

Finally there is an equation left to consider. Because the converter operates following the II control model, v_{dc} is part of the data. It has to be treated similarly to a PV bus of a classical AC grid. The absolute value is known but its phase not yet.

$$W = |V_2|^2, \quad (3)$$

where W is a given value.

At this stage of the formulation, the system of equations constituted by (1), (2) and (3) appears to be nonlinear. Consequently, an iterative method like the well-known Newton-Raphson could be employed. Nevertheless, this paper will present a formulation based on the holomorphic embedding method. No paper covers the AC/DC conversion with that last approach, and on the other hand, the FGBM allows the usage of Sigma approximants to diagnose the state of the system.

III. EMBEDDING

The holomorphic embedding method is based on embedding the equations involved. Embedding means that the problem is submerged inside a bigger problem. After a reference state is obtained, the solution can be extended up to the operative state. The choice of embedding is not unique. Despite that, the canonical embedding is a tested alternative that works adequately. It states that $V_i[0] = 1 \ \forall i$ and $I_i[0] = 0 \ \forall i$.

Therefore, (1) develops into

$$I_f(s) = y_s V_2(s) - y_s V_1(s) + s j \frac{b_c}{2} V_2(s) + s j B_{eq}(s) V_2(s) + s G |I_f(s)|^2 V_2(s). \quad (4)$$

Note that only $I_f(s)$ and the terms including y_s do not multiply directly by s . This way they are the responsible for

conforming the reference state. $V_1(s)$ responds to the typical embedding for slack buses

$$V_1(s) = 1 + s(V_1 - 1), \quad (5)$$

where V_1 is the known voltage with the reference angle set at 0. It is convenient to expand (4) further to avoid $|I_f(s)|^2$

$$I_f(s) = y_s V_2(s) - y_s V_1(s) + s j \frac{b_c}{2} V_2(s) + s j B_{eq}(s) V_2(s) + s G I_f^{(re)}(s) I_f^{(re)}(s) I_f^{(im)}(s) I_f^{(im)}(s) V_2(s), \quad (6)$$

where $I_f^{(re)}(s)$ and $I_f^{(im)}(s)$ are the real and imaginary part of $I_f(s)$ respectively.

When it comes to (2), the variables should also be fragmented into real and imaginary part.

$$sP + 0j = (V_2^{(re)}(s) + jV_2^{(im)}(s))(I_f^{(re)}(s) - jI_f^{(im)}(s)). \quad (7)$$

This way the resulting system of equations will not be concerned with obtaining the absolute value and the phases like the Newton-Raphson would. Instead, the real and imaginary parts will be computed akin to the traditional holomorphic embedding method.

Lastly, (3) adopts the form

$$1 + s(W - 1) = V_2^{(re)}(s)V_2^{(re)}(s) + V_2^{(im)}(s)V_2^{(im)}(s). \quad (8)$$

From (6), (7) and (8) it can be checked that all these equations are compatible with the desired reference state. Moreover, the c term that builds $B_{eq}(s)$ will be obtained at the same time the $c+1$ coefficient of the other variables is obtained. In other words, its calculation will always be a step behind.

A system of 5 equations is derived from (6), (7) and (8), since the first two are complex a generalized system at depth c becomes

$$\begin{pmatrix} 1 & 0 & -g & b & 0 \\ 0 & 1 & -b & -g & -1 \\ 1 & 0 & 0 & 0 & 0 \\ 0 & 1 & 0 & 0 & 0 \\ 0 & 0 & 2 & 0 & 0 \end{pmatrix} \begin{pmatrix} I_f^{(re)}[c] \\ I_f^{(im)}[c] \\ V_2^{(re)}[c] \\ V_2^{(im)}[c] \\ B_{eq}[c-1] \end{pmatrix} = RHS[c], \quad (9)$$

where it has already been considered that $V_2[0] = 1$. It only remains to construct the RHS vector. The terms that intervene in (6) and build RHS at the first stage turn out to be

$$A = -g(V_1 - 1) + G V_2[0] \left(I_f^{(re)}[0]^2 + I_f^{(im)}[0]^2 \right) - b(V_1 - 1) + j \frac{b_c}{2} V_2[0], \quad (10)$$

where $g + jb = y_s$. From here

$$RHS[1] = \begin{pmatrix} \Re[A] \\ \Im[A] \\ P \\ 0 \\ W - 1 \end{pmatrix}. \quad (11)$$

As a result of that, in order to obtain the first set of coefficients the matrix of (9) has to be inverted (or factorized). In contrast

to the Newton-Raphson scheme, here the matrix remains the same, independent of the order. From a computational time standpoint, although the holomorphic embedding method usually needs between 20 and 40 coefficients, each of its step is essentially faster than a Newton-Raphson iteration.

For a generalized order $c \geq 2$ the *RHS* expressions gain in complexity. For (6)

$$\begin{aligned} A = & G \sum_{k=0}^{c-1} V_2[k] \sum_{j=0}^{c-1-k} I_f^{(re)}[j] I_f^{(re)}[c-1-k-j] \\ & + G \sum_{k=0}^{c-1} V_2[k] \sum_{j=0}^{c-1-k} I_f^{(im)}[j] I_f^{(im)}[c-1-k-j] \quad (12) \\ & + j \left(\frac{b_c}{2} V_2[c-1] + \sum_{k=1}^{c-1} V_2[k] B_{eq}[c-1-k] \right), \end{aligned}$$

where there are some double convolutions which are not worrying in the sense that the algorithm can still converge to the sought solution.

Then, the real part of (7) is converted into

$$B = - \sum_{k=1}^{c-1} V_2^{(re)}[k] I_f^{(re)}[c-k] - \sum_{k=1}^{c-1} V_2^{(im)}[k] I_f^{(im)}[c-k], \quad (13)$$

while the imaginary becomes

$$C = - \sum_{k=1}^{c-1} V_2^{(im)}[k] I_f^{(re)}[c-k] - \sum_{k=1}^{c-1} V_2^{(re)}[k] I_f^{(im)}[c-k]. \quad (14)$$

Finally, there is only one expression left to consider. From (8) the expansion of coefficients yields

$$D = - \sum_{k=1}^{c-1} V_2^{(re)}[k] V_2^{(re)}[c-k] - \sum_{k=1}^{c-1} V_2^{(im)}[k] V_2^{(im)}[c-k]. \quad (15)$$

All this allows the construction of the definitive *RHS* vector

$$RHS[c] = \begin{pmatrix} \Re[A] \\ \Im[A] \\ B \\ C \\ D \end{pmatrix}. \quad (16)$$

Thus, the algorithm has been fully built for any given order. Of course it would change depending on the dimensions of the system as well as the variables to control, but its core remains. From (9) it can be seen that the dependence of g and b with the voltages is similar to the one encountered with AC systems, despite having changed the signs here.

IV. RESULTS

To show that the holomorphic embedding is compatible with the FGBM some basic results are offered. The first and most convenient test to implement has to do with the errors and how they evolve according to the chosen depth. This alone is often enough to get a glimpse of the convergence properties of the series. An embedding that leads to convergent series

is more appropriate than another that does not. However, both can generate a final correct solution.

Table I captures the initial dataset of the problem expressed in per unit values.

TABLE I
DATA OF THE SIMPLE AC/DC SYSTEM

Magnitude	Value
P	-0.2
V_1	1.05
W	0.95
g	5
b	-10
G	10
b_c	100

A negative P value symbolizes active power demand. It has to be noted that all these numbers are made up and could be not totally congruent with the current real-life systems and converters.

Figure 2 plots the maximum error as a function of the number of coefficients used, both with Padé approximants and directly summing the terms. In this state the convergence properties are so favorable that Padé approximants do not provide any substantial advantage. From 25 coefficients onwards the error plateaus. Double-precision floating-point format was employed.

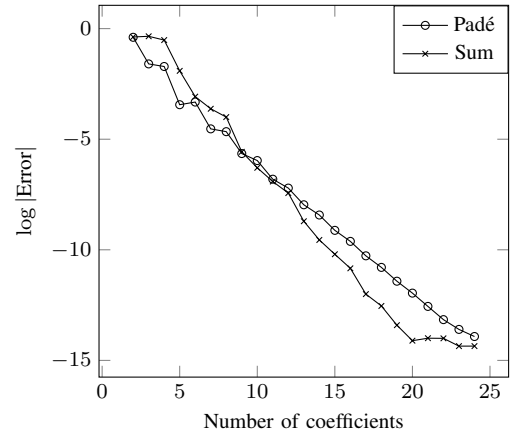


Fig. 2. Maximum error depending on the depth

It is worth-telling that other models for the AC/DC conversion could also be used. however, the traditional ones as presented in [5]- [9] when combined with the holomorphic embedding do not yield convergent results. In addition to that, it is hard to find a suitable embedding. Hence the relevance of the FGBM.

Another representative result is the maximum power the DC load can consume so that the power flow is still feasible. As expected, the error should increase. Figure 3 plots the maximum error as a function of P with a depth of 30 terms.

From what can be observed, for $|P| < 0.3$ the error obtained with Padé or with the sum remains practically the same. Padé approximants become handy once $|P|$ increases. Despite

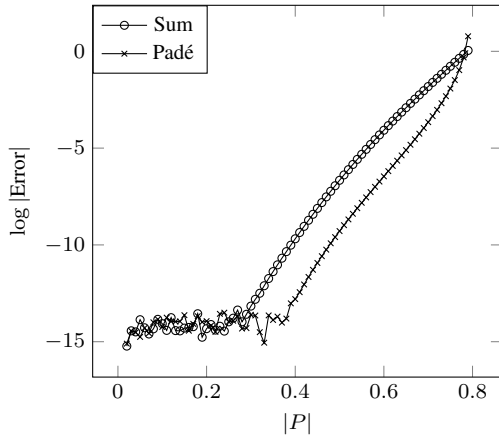


Fig. 3. Maximum error depending on the active power load

following the same trend, its maximum error stays about 2 orders of magnitude below the one with the summation of coefficients.

It is also valuable to evaluate the variation of B_{eq} depending on variations of P . Table II displays its value according to the selected $|P|$. The closer to 0 $|P|$ is, the smaller B_{eq} gets. All in all, there is a weak link between these two variables.

TABLE II
 B_{eq} VALUES AS A FUNCTION OF P

P	B_{eq}
0.6	-48.86
0.4	-50.29
0.2	-50.86
-0.2	-50.65
-0.4	-49.73
-0.6	-47.50

V. CONCLUSION

A functional combination of the holomorphic embedding method with the AC/DC power flow has been achieved for a simple test case where the series involved converged at a fast pace. The FGBM turns out to be an innovative adequate model which facilitates the combination of the AC power flow with the DC power flow with no need to decouple systems.

This paper lands the foundation of the development of a full algorithm based on the holomorphic embedding able to solve realistic AC/DC systems. That would benefit from the resources that the holomorphic embedding offers: Thévenin approximants to plot accurate PV curves, Sigma approximants to diagnose the system and the Padé-Weierstrass to improve the solution when needed. The robustness of the holomorphic embedding is arguably greater than iterative methods, making it a possible ground-breaking tool to be applied in the AC/DC power flow.

REFERENCES

[1] E. Bompard, G. Fulli, M. Ardelean, M. Masera. "It's a bird it's a plane it's a... Supergrid!: Evolution opportunities and critical issues for Pan-European transmission", in *IEEE Power and Energy Magazine*, vol. 12, no. 2, pp. 40-40, February 2014.

[2] D. Van Hertem, O. Gomis-Bellmunt, J. Liang. "HVDC Grids: For Offshore and Supergrid of the Future". Wiley-IEEE Press. 2016.

[3] A. Alvarez Bustos, B. Kazemtabrizi. "Flexible General Branch Model Unified Power Flow Algorithm for Future Flexible AC/DC Networks", in 2018 IEEE International Conference on Environment and Electrical Engineering and 2018 IEEE Industrial and Commercial Power Systems Europe (EEEIC / ICPS Europe): 12-15 June 2018, Palermo, Italy. Conference proceedings. Piscataway, NJ: IEEE.

[4] A. Trias. "HELM: The Holomorphic Embedding Load-Flow Method". 2012 IEEE Power and Energy Society General Meeting, San Diego, California, 2012, pp. 1-8.

[5] D. J. Tylavsky, "A Simple Approach to the Solution of the ac-dc Power Flow Problem", in *IEEE Transactions on Education*, vol. 27, no. 1, pp. 31-40, February 1984.

[6] J. Arrillaga, P. Bodger. "A.C.-d.c. load flows with realistic representation of the converter plant", in *Proceedings of the Institution of Electrical Engineers*, vol. 125, no. 1, pp. 41-46, January 1978.

[7] J. Arrillaga, C. P. Arnold, J. R. Camacho, S. Sankar. "AC-DC Load Flow with Unit Connected Generator-Converter Infeeds", in *IEEE Transactions on Power Systems*, vol. 8, no. 2, pp. 701-706, May 1993.

[8] J. Arrillaga, C. P. Arnold. "Computer Analysis of Power Systems". John Wiley and Sons. 1994.

[9] B. Yang, L. Chuang, L. Zhu, C. Guo, Z. Gu and Z. Wang, "AC/DC Power Flow Algorithm Considering Various Controls Transformation," in *2018 2nd IEEE Conference on Energy Internet and Energy System Integration (EI2)*, Beijing, 2018, pp. 1-5.

[10] A. Trias and J. L. Marín, "The Holomorphic Embedding Loadflow Method for DC Power Systems and Nonlinear DC Circuits," in *IEEE Transactions on Circuits and Systems I: Regular Papers*, vol. 63, no. 2, pp. 322-333, Feb. 2016.

[11] A. Trias. HELM: *The Holomorphic Embedding Load-Flow Method*. Foundations and Implementations. Foundations and Trends® in Electric Energy Systems, vol. 3, no. 3-4, pp. 140-370, 2018.

[12] U. Sur, A. Biswas, J. N. Bera and G. Sarkar, "Holomorphic Embedding Load Flow Modeling of DSTATCOM for Active Distribution Networks," *2020 IEEE Calcutta Conference (CALCON)*, Kolkata, India, 2020, pp. 435-438.

[13] P. Singh and R. Tiwari, "STATCOM Model Using Holomorphic Embedding," in *IEEE Access*, vol. 7, pp. 33075-33086, 2019.